Vol 446 | 29 March 2007 | doi:10.1038/nature05647

Fluctuating valence in a correlated solid and the anomalous properties of δ-plutonium

J. H. Shim[1], K. Haule[1] & G. Kotliar[1]

Although the nuclear properties of the late actinides (plutonium, americium and curium) are fully understood and widely applied to energy generation, their solid-state properties do not fit within standard models and are the subject of active research[1]. Plutonium displays phases with enormous volume differences, and both its Pauli-like magnetic susceptibility and resistivity are an order of magnitude larger than those of simple metals[2]. Curium is also highly resistive, but its susceptibility is Curie-like at high temperatures and orders antiferromagnetically[3] at low temperatures. The anomalous properties of the late actinides stem from the competition between itinerancy and localization of their *f*-shell electrons, which makes these elements strongly correlated materials. A central problem in this field is to understand the mechanism by which these conflicting tendencies are resolved in such materials. Here we identify the electronic mechanisms responsible for the anomalous behaviour of late actinides, revisiting the concept of valence using a theoretical approach that treats magnetism, Kondo screening, atomic multiplet effects and crystal field splitting on the same footing. We find that the ground state in plutonium is a quantum superposition of two distinct atomic valences, whereas curium settles into a magnetically ordered single valence state at low temperatures. The f^7 configuration of curium is contrasted with the multiple valences of the plutonium ground state, which we characterize by a valence histogram. The balance between the Kondo screening and magnetism is controlled by the competition between spin–orbit coupling, the strength of atomic multiplets and the degree of itinerancy. Our approach highlights the electronic origin of the bonding anomalies in plutonium, and can be applied to predict generalized valences and the presence or absence of magnetism in other compounds starting from first principles.

To understand the unique properties of elemental plutonium and its distinctive placement in the periodic table, it is essential to build a theory of actinides that can describe itinerant actinides as well as late actinides beyond plutonium. In the late rare-earth materials, the spin–orbit coupling and the hybridization is weak. The direct exchange promotes a ferromagnetic Kondo interaction between the *spd* and *f* electrons that results in a decoupling of *spd* and *f* electrons at low energies. In the late actinides the net Kondo interaction is antiferromagnetic, leading to strong correlation phenomena such as anomalously high room-temperature resistivities[4]. Curium, which follows americium in the periodic table, provides a very useful analogue to plutonium expanded beyond the equilibrium volume of its δ-phase. Curium is obtained by adding an electron to americium's inert *5f* shell (total angular momentum $J = 0$), while plutonium is obtained by creating a hole in the shell. The ability to predict magnetism in curium and its absence in plutonium is a strong test for our methodology, and we will use it as a benchmark for the quality of our theory of actinides.

To treat realistic multiplets and band structure, we use a new implementation of the merger of the local density approximation and the dynamical mean field theory (LDA+DMFT)[5,6]. The DMFT method requires a solution of a quantum impurity problem which was here accomplished by an accurate impurity solver (which employed a vertex corrected one-crossing approximation[6]) and the results were further crosschecked against a continuous time quantum Monte Carlo method[7,8]. We treat the full atomic physics (all the Slater integrals F_0, F_2, F_4 and F_6) on the same footing with the realistic band structure obtained by the relativistic version of the linear muffin-tin orbital method[9]. This LDA+DMFT approach treats magnetism and Kondo physics on an equal footing, and takes into account all the multiplet structure and crystal fields. As in all the earlier studies[10] we take Coulomb interaction $U = 4.5$ eV and we compute the rest of the Slater integrals (F_2, F_4 and F_6) from atomic physics[11], which, following the usual practice, are rescaled to 80% of their value.

Underlying the dynamical mean field approach[5] is a physical picture in which the *f* electrons fluctuate among the different atomic configurations by exchanging electrons with a reservoir. The properties of the reservoir are determined self-consistently from the knowledge of the local spectral function. The self-consistency condition allows solutions with partially delocalized *f* electrons forming quasiparticle bands, but at the same time, the *f* electrons are allowed to preserve their atomic character for a short period of time, which leads to formation of Hubbard bands in the spectral function. When the *f* electrons get sufficiently localized, magnetic solutions are possible and become more energetically favourable than paramagnetic solutions at low temperature.

The fingerprint of strong correlations is encoded in the many-body self-energy, which becomes a 14×14 matrix dependent on frequency ω but not momentum $\mathbf{k}$. Adding this to the hamiltonian matrix, which also contains *spd* electrons, gives rise to the Green's function of the problem, $G(\omega,\mathbf{k})$. Integrated over momentum, it results in the local spectral function, which is measured in photoemission and inverse photoemission experiments.

To investigate phases with antiferromagnetic long-range order, the self-energy is allowed to be spin dependent, and the lattice is partitioned into two different sublattices, A and B, which experience different environments. The solution of two single impurity problems, coupled through the self-consistency condition, gives the self-energies in both sublattices A and B (ref. 5). We start from a magnetic state where the effective mediums for the different projections of the *z* component of the electron total angular momentum j_z at the A and B sublattices are different, and we watch how they evolve under iteration. We find that plutonium does not take advantage of the possibility of a broken symmetry and hence is non-magnetic, whereas curium does.

Starting from a general initial condition, upon iteration the plutonium spectral functions converge to a j_z independent spectral

---

[1]Department of Physics and Astronomy and Center for Condensed Matter Theory, Rutgers University, Piscataway, New Jersey 08854-8019, USA.

function. On the other hand, curium has 14 non-equivalent spectral functions, reflecting the low-temperature antiferromagnetism, as displayed in Fig. 1. Notice the Hubbard bands, atomic-like features, and the Kondo resonance, which is present in plutonium but not in curium. Multiplet effects are clearly visible and provide widths to the Hubbard bands, as pointed out previously in studies of americium[12]. Here we show that they play an even more important role in determining the renormalized Fermi energy, or the Kondo scale. For plutonium we obtain a Kondo energy of the order of 800 K, which compares favourably with the measured specific heat of the order of 60 mJ mol^{-1} K^{-1} (ref. 13). Turning off the Hund's rule coupling, which is possible theoretically but not experimentally, would result in a much larger Kondo energy in plutonium and in a non-magnetic heavy fermion state in curium in disagreement with experiments. Hence the Hund's rule coupling plays an unexpected role in the actinide series, renormalizing down the Kondo energy. Although the *f*–*spd* hybridization and the *f*–*f* hopping is larger in actinides than in lanthanides, it is still much smaller than the correlation strength in the form of the Hubbard interaction, and the width of the Hubbard bands is the result of the multiplet splitting, rather than coherent propagation, unlike the Kohn Sham bands in the standard model of solids.

To define valence, we focus on the reduced density matrix of the *f* states at a given site, which is obtained from the exact density matrix of the solid by tracing over all degrees of freedom except for those of the 5*f* shell at a given site (see Supplementary Information). The eigenvalues of this reduced density matrix give the probability of observing different *f*-electron atomic configurations at a given unit cell associated with an actinide nucleus. The solution of the DMFT impurity model allows us to visualize the *f* electrons as fluctuating between various atomic configurations and exchanging electrons with the surrounding medium. As a function of time, the *f* electrons in the atom change their atomic configuration while absorbing and emitting electrons into the medium. We keep track of the different atomic configurations visited and draw them as histograms, which give complementary information to the photoemission spectra. These histograms for δ-plutonium and curium are presented in Fig. 2. Notice that plutonium does not have a well defined valence; its *f* electrons live a double life, spending considerable time in several atomic configurations, even though plutonium's average *f* electron count is close to $5f^5$. We describe this situation with a histogram which is peaked for a few atomic eigenstates, including atomic ground states of $5f^5$ and $5f^6$. The system is in a mixed valence state[14] with an average *f* occupation of $n_f \approx 5.2$. In curium the *f* electrons are locked into one $5f^7$ dominant configuration, and the histogram is peaked only for the ground state of the atom.

X-ray absorption spectroscopy and electron energy-loss spectroscopy from the core 4*d* states are powerful probes of the valence. The strong spin–orbit coupling of the core states gives rise to two spin–orbit split absorption lines, representing $4d_{5/2} \rightarrow 5f$ and $4d_{3/2} \rightarrow 5f$ transitions[15]. The branching ratio *B*, that is, the relative strength of the $4d_{5/2}$ absorption, is a measure of the strength of the spin–orbit coupling interaction in the *f* shell. Ignoring the electrostatic interaction between core and valence electrons, known to be negligible in plutonium[16], results in the following general expression obtained first by Van der Laan and collaborators[15]:

$$B = \frac{A_{5/2}}{A_{5/2} + A_{3/2}} = \frac{3}{5} - \frac{4}{15}\frac{1}{14 - <n_{5/2}> - <n_{7/2}>} \sum_{i \in f} < \mathbf{l}_i \cdot \mathbf{s}_i > \tag{1}$$

$$\sum_{i \in f} < \mathbf{l}_i \cdot \mathbf{s}_i > = \frac{3}{2} < n_{7/2} > - 2 < n_{5/2} >$$

where $A_{5/2}$ and $A_{3/2}$ are associated with area under the peaks corresponding to $4d_{5/2} \rightarrow 5f$ and $4d_{3/2} \rightarrow 5f$ transitions, respectively. The term $\sum_{i \in f} < \mathbf{l}_i \cdot \mathbf{s}_i >$ measures the strength of the spin–orbit coupling

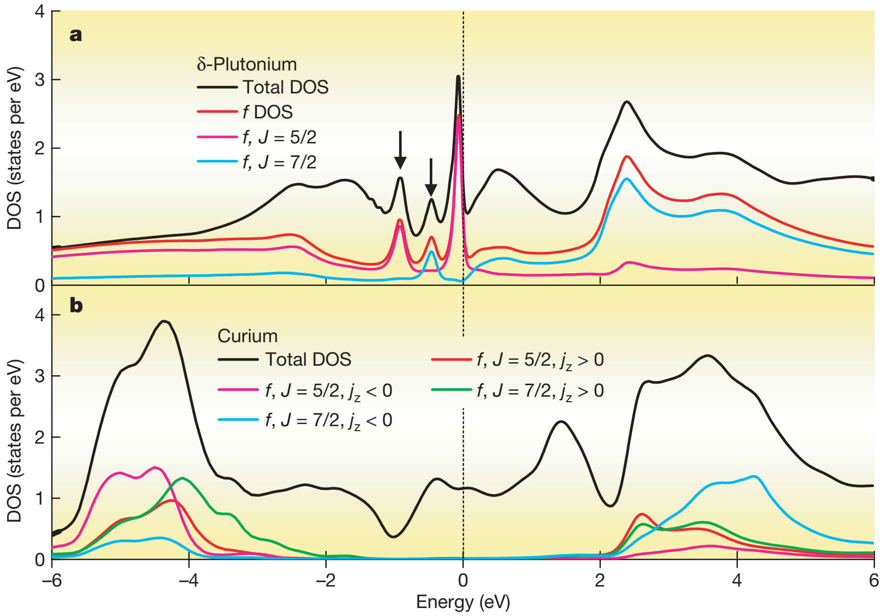

Figure 1 | The spectral functions of δ-plutonium and face-centred-cubic curium. a, δ-Plutonium is in a paramagnetic state with its moment totally screened by the Kondo effect, which is observed as a resonance at the Fermi level in the *f* spectra. In addition to the broad Hubbard band and sharp Kondo peak, two additional peaks below the Fermi level appear in our spectral function (marked with arrows), which were recently identified in photoemission experiments[28–30]. The virtual charge fluctuations are primarily between the blue central peak in Fig. 2 (ground state of the atomic sector with $N_f = 5$ atoms) and the green side peak $|N_f = 6, J = 0, \gamma = 0\rangle$ (ground state of $N_f = 6$) in the same panel; γ is defined in Fig. 2 legend. The two arrowed sub-bands around 0.5 and 0.85 eV come mostly from the charge fluctuations between the second blue peak $|N_f = 5, J = 7/2, \gamma = 0\rangle$ and the ground state of $N_f = 6$, and between $|N_f = 5, J = 5/2, \gamma = 1\rangle$ and the same ground state of $N_f = 6$, respectively. They disappear above the coherence temperature, so they are part of the coherent many-body spectra. **b**, The curium spectral function in the antiferromagnetic state. The diagonal components of the 14 × 14 matrix spectral function are shown separately for the positive and negative components of the electron spin j_z. The theoretical total density of states (DOS) displays the experimentally observed features at approximately the same energies, and calls for more detailed comparisons with experiment, which would require incorporating the photoemission matrix elements into the theory.

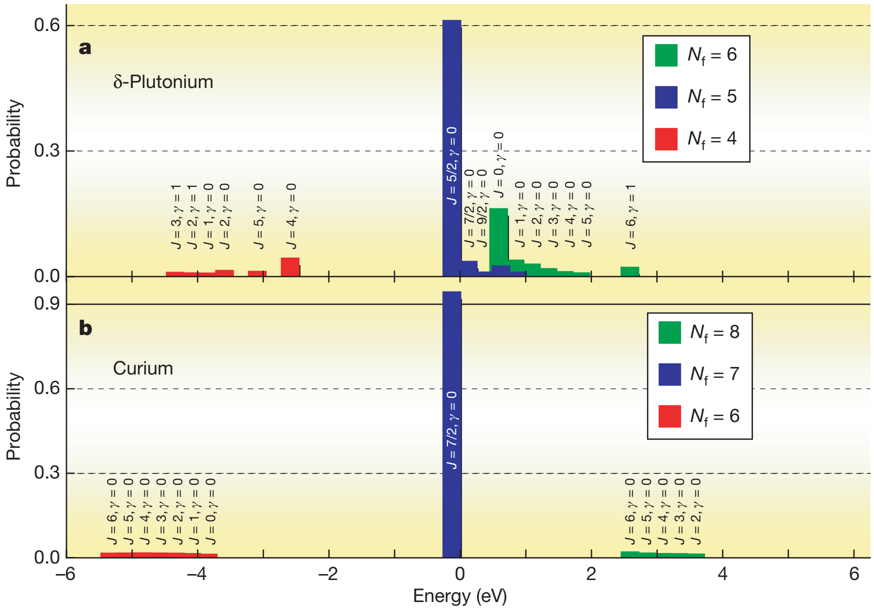

Figure 2 | Projection of the DMFT ground state to various atomic configurations. The histograms describe the generalized concept of valence, where the *f* electron in the solid spends appreciable time in a few atomic configurations. The height of the peak corresponds to the fraction of the time the *f* electron of the solid spends in one of the eigenstates of the atom, denoted by the total spin *J* of the atom. We summed up the probabilities for the atomic states that differ only in the *z* component of the total spin J_z. The rest of the atomic quantum numbers are grouped into a single quantum number $\gamma = 0, 1, \ldots$. The *x* axis indicates the energy of the atomic eigenstates defined by: $\text{energy}(N_f - 1, J\gamma) = E_{\text{atom}}(N_f, \text{ground state}) - E_{\text{atom}}(N_f - 1, J\gamma)$ and $\text{energy}(N_f + 1, J\gamma) = E_{\text{atom}}(N_f + 1, J\gamma) - E_{\text{atom}}(N_f, \text{ground state})$, where N_f is 5 and 7 for δ-plutonium and curium, respectively.

in the valence *f* states, and $n_{5/2}$ and $n_{7/2}$ are averaged partial occupations of the *f* valence states.

Comparison of measured branching ratios in actinides[17] with atomic physics computations[16] indicated the important role of spin–orbit coupling and gave strong evidence in favour of a $5f^5$ configuration. We now evaluate *B* for both curium and plutonium, using DMFT, which goes beyond atomic physics by incorporating the effects of itinerancy and multiple valences. The DMFT results are summarized in Table 1 and are compared with experiment[17] where available. We stress the importance of first principles calculations including spin–orbit coupling, itinerancy and multiplet effects, as these are competing effects. Whereas the spin–orbit coupling increases faster than the Hund's coupling (Slater F_2) with increasing number of *f* electrons, the changes in the degree of itinerancy are of comparable magnitude and affect the relative strength of the effective spin–orbit coupling compared to the Hund's coupling and crystal fields. As a result, the effective spin–orbit coupling is smaller in curium than plutonium, placing curium much closer to the Russell-Saunders (*L*–*S*) coupling than plutonium[18] (see last column in Table 1). The resulting curium moment $\mu \approx 2\sqrt{S(S+1)} \approx 7.9\mu_B$ (where μ_B is the Bohr magneton and *S* is the spin) is close to the observed experimental value[3], which is clearly incompatible with *j*–*j* coupling (one $f_{7/2}$ electron would result in a moment of $l + 2s = 3 + 1\ \mu_B$).

We now contrast our findings with earlier approaches. Spin density functional theory (SDFT) calculations predict that all late actinides (plutonium, americium and curium) are magnetic, with large ordered magnetic moments of the order of a few μ_B (ref. 19). Experimentally, it is now established that no fluctuating or ordered moments exist in metallic plutonium[2] and americium[20], whereas curium orders magnetically with a large magnetic moment. SDFT can be viewed as a form of static mean-field theory, which is known to sometimes produce spurious magnetic states in order to mimic the effect of correlations.

Other theories of plutonium posit that in this material some 5*f* electrons are localized and some are itinerant. The mixed level model[21] assumes that four electrons are localized, that is, condensed into an atomic like singlet, while one *f* electron is itinerant. In the self-interaction corrected LDA, the valence of the *f* is frozen, and the total energy is determined for each valence to select the one with the lowest total energy. The latter approach[22] finds that configurations with four, three, two, one or zero localized 5*f* electrons are almost degenerate. This can be taken as an indication that the dynamical treatment of valence presented in this Letter is needed for plutonium.

Other calculations (LDA+U[23,24], DMFT-FLEX[25]) suggest that plutonium is close to an inert $5f^6$ configuration with a singlet formed out of six localized *f* electrons. A non-magnetic configuration naturally accounts for the absence of moments in plutonium, but is too inert to account for the fact that the specific heats in α and δ phases differ by more than a factor of two[2]. Furthermore, X-ray absorption experiments[26] and photoemission on thin plutonium layers[27], as well as previous DMFT calculations for plutonium[10], are very suggestive that the *f* electrons are close to $5f^5$ configuration.

The full dynamic treatment of multiplets and Kondo physics, carried out in this Letter, brings a significant admixture of $5f^6$ valence, establishing continuity with weak coupling treatments[25], while accounting for the mass enhancement in α- and δ-plutonium. Our technical and conceptual advances in understanding δ-plutonium and curium lead to several experimental predictions. In the paramagnetic state, the volume enclosed by the Fermi surface of plutonium should contain an even number of electrons, whereas that of curium should contain an odd number of electrons, that is, its three *spd* electrons. These predictions can be tested by de Haas–van Alphen experiments or angle-resolved photoemission experiments. Furthermore, the physical picture of plutonium as a mixed-valence metal provides a natural explanation for the large sensitivity of its volume to small changes in temperature, pressure or doping. Moreover, the

Table 1 | Branching ratio

	f count	$B_{\text{DMFT theory}}$	B_{exp} (ref. 16)	$B_{L\text{-}S}$	B_{jj}	$(B_{\text{DMFT}} - B_{L\text{-}S})/(B_{jj} - B_{LS})$
δ-Plutonium	5.2	0.83	0.847	0.69	0.90	0.67
Curium	7.0	0.75		0.6	1.0	0.38

The *f*-electron count and branching ratio, *B*, of the $4d \rightarrow 5f$ edge spectra of δ-plutonium and curium. $B_{L\text{-}S}$ and B_{jj} correspond to limiting cases of the pure Russell-Saunders and *j*–*j* coupling, respectively.

mixed-valence nature of plutonium can be probed by optical conductivity experiments, which should display a hybridization gap on a scale corresponding to several times the Kondo energy. In addition to the standard low-energy Drude peak, the optical conductivity should display a hybridization dip around $1{,}000\,\mathrm{cm}^{-1}$ and a broad mid-infrared peak between 3,000 and $4{,}000\,\mathrm{cm}^{-1}$. The one-electron spectra and the X-ray branching ratio of curium are further quantitative theoretical predictions, which can be tested experimentally via photoemission and X-ray absorption measurements.

Finally, the use of DMFT for extracting valence histograms and thinking about mixed valences should have applications for many other strongly correlated compounds. Two pressing examples are UO_2 and PuO_2 (important by-products in nuclear reactors), whose valence properties are not well understood.

Received 2 November 2006; accepted 26 January 2007.

1. Lander, G. Sensing electrons on the edge. *Science* **301,** 1057–1059 (2003).
2. Lashley, J. C., Lawson, A., McQueeney, R. J. & Lander, G. H. Absence of magnetic moments in plutonium. *Phys. Rev. B* **72,** 054416 (2005).
3. Huray, P. G., Nave, S. E., Peterson, J. R. & Haire, R. G. The magnetic susceptibility of ^{248}Cm metal. *Physica B* **102,** 217–220 (1980).
4. Brodsky, M. B. Magnetic properties of the actinide elements and their metallic compounds. *Rep. Prog. Phys.* **41,** 1547–1608 (1978).
5. Georges, A., Kotliar, G., Krauth, W. & Rozenberg, M. J. Dynamical mean-field theory of strongly correlated fermion systems and the limit of infinite dimensions. *Rev. Mod. Phys.* **68,** 13–125 (1996).
6. Kotliar, G. *et al.* Electronic structure calculations with dynamical mean-field theory. *Rev. Mod. Phys.* **78,** 865–951 (2006).
7. Werner, P., Comanac, A., de' Medici, L., Troyer, M. & Millis, A. J. Continuous-time solver for quantum impurity models. *Phys. Rev. Lett.* **97,** 076405 (2006).
8. Haule, K. Quantum Monte Carlo impurity solver for cluster DMFT and electronic structure calculations in adjustable base. Preprint at ⟨http://arxiv.org/cond-mat/0612172⟩ (2006).
9. Savrasov, S. Y. Linear-response theory and lattice dynamics: A muffin-tin-orbital approach. *Phys. Rev. B* **54,** 16470–16486 (1996).
10. Savrasov, S. Y., Kotliar, G. & Abrahams, E. Correlated electrons in δ-plutonium within a dynamical mean-field picture. *Nature* **410,** 793–795 (2001).
11. Cowan, R. D. *The Theory of Atomic Structure and Spectra* (Univ. California Press, Berkeley, 1981).
12. Savrasov, S. Y., Haule, K. & Kotliar, G. Many-body electronic structure of americium metal. *Phys. Rev. Lett.* **96,** 036404 (2006).
13. Lashley, J. C. *et al.* Experimental electronic heat capacities of α- and δ-plutonium: Heavy-fermion physics in an element. *Phys. Rev. Lett.* **91,** 205901 (2003).
14. Varma, C. M. Mixed-valence compounds. *Rev. Mod. Phys.* **48,** 219–238 (1976).
15. Thole, B. T. & van der Laan, G. Linear relation between x-ray absorption branching ratio and valence-band spin-orbit expectation value. *Phys. Rev. A* **38,** 1943–1947 (1988).
16. van der Laan, G. *et al.* Applicability of the spin-orbit sum rule for the actinides 5f states. *Phys. Rev. Lett.* **93,** 097401 (2004).
17. Moore, K. T., van der Laan, G., Haire, R. G., Wall, M. A. & Schwartz, A. J. Oxidation and aging in U and Pu probed by spin-orbit sum rule analysis: Indications for covalent metal-oxide bonds. *Phys. Rev. B* **73,** 033109 (2006).
18. Moore, K. T. *et al.* Failure of Russell-Saunders coupling in the 5*f* states of plutonium. *Phys. Rev. Lett.* **90,** 196404 (2003).
19. Solovyev, I. V., Liechtenstein, A. I., Gubanov, V. A., Antropov, V. P. & Andersen, O. K. Spin-polarized relativistic linear-muffin-tin-orbital method: Volume-dependent electronic structure and magnetic moment of plutonium. *Phys. Rev. B* **43,** 14414–14422 (1991).
20. Kanellakopulos, B., Blaise, A., Fournier, J. M. & Müeller, W. The magnetic susceptibility of americium and curium metal. *Solid State Commun.* **17,** 713–715 (1975).
21. Wills, J. M. *et al.* A novel electronic configuration of the 5f states in δ-plutonium as revealed by the photo-electron spectra. *J. Electron Spectrosc. Relat. Phenom.* **135,** 163–166 (2004).
22. Svane, A., Petit, L., Szotek, Z. & Temmerman, W. M. Self-interaction corrected local spin density theory of 5f electron localization in actinides. Preprint at ⟨http://arxiv.org/cond-mat/0610146⟩ (2006).
23. Shorikov, A. O., Lukoyanov, A. V., Korotin, M. A. & Anisimov, V. I. Magnetic state and electronic structure of the δ and α phases of metallic Pu and its compounds. *Phys. Rev. B* **72,** 024458 (2005).
24. Shick, A. B., Drchal, V. & Havela, L. Coulomb-*U* and magnetic-moment collapse in δ-Pu. *Europhys. Lett.* **69,** 588–594 (2005).
25. Pourovskii, L. V. *et al.* Nature of non-magnetic strongly-correlated state in δ-plutonium. *Europhys. Lett.* **74,** 479–485 (2006).
26. Tobin, J. G. *et al.* Competition between delocalization and spin-orbit splitting in the actinide 5f states. *Phys. Rev. B* **72,** 085109 (2005).
27. Gounder, T., Havela, L., Wastin, F. & Rebizant, J. Evidence for the 5*f* localisation in thin Pu layers. *Europhys. Lett.* **55,** 705–711 (2001).
28. Arko, A. J. *et al.* Electronic structure of α- and δ-Pu from photoelectron spectroscopy. *Phys. Rev. B* **62,** 1773–1779 (2000).
29. Gouder, T., Eloirdi, R., Rebizant, J., Boulet, P. & Huber, F. Multiplet structure in Pu-based compounds: A photoemission case study of $PuSi_x$ ($0.5 \leq x \leq 2$) films. *Phys. Rev. B* **71,** 165101 (2005).
30. Tobin, J. G. *et al.* Resonant photoemission in *f*-electron systems: Pu and Gd. *Phys. Rev. B* **68,** 155109 (2003).

Supplementary Information is linked to the online version of the paper at www.nature.com/nature.

Acknowledgements This work was supported by the Basic Energy Science division of the DOE. J.H.S. acknowledges a grant from the Korean Research Foundation.

Author Information Reprints and permissions information is available at www.nature.com/reprints. The authors declare no competing financial interests. Correspondence and requests for materials should be addressed to K.H. (haule@physics.rutgers.edu).